FINAL FOCUS ION BEAM INTENSITY FROM TUNGSTEN FOIL CALORIMETER AND SCINTILLATOR IN NDCX-I*

S.M. Lidia#, F. Bieniosek, E. Henestroza, P. Ni, P. Seidl, LBNL, Berkeley, CA 94720, U.S.A.

Abstract

Laboratory high energy density experiments using ion beam drivers rely upon the delivery of high-current, high-brightness ion beams with high peak intensity onto targets. Solid-state scintillators are typically used to measure the ion beam spatial profile but they display dose-dependent degradation and aging effects. These effects produce uncertainties and limit the accuracy of measuring peak beam intensities delivered to the target. For beam tuning and characterizing the incident beam intensity, we have developed a cross-calibrating diagnostic suite that extends the upper limit of measurable peak intensity dynamic range. Absolute intensity calibration is obtained with a 3μm thick tungsten foil calorimeter and streak spectrometer. We present experimental evidence for peak intensity measures in excess of 400 kW/cm^2 using a 0.3 MV, 25 mA, 5-20 μsec K^{+1} beam. Radiative models and thermal diffusion effects are discussed because they affect temporal and spatial resolution of beam intensity profiles.

INTRODUCTION

The US Heavy Ion Fusion Science program is developing techniques for heating ion-beam-driven warm dense matter (WDM) targets [1-3]. Ion beams have several attractive features as drivers for generating WDM conditions:

- Precise control of local beam energy deposition *dE/dx*, nearly uniform throughout a volume, and not strongly affected by target temperature,
- Ability to use large sample sizes (~1 μm thick by 1 mm diameter),
- The ability to heat any target material: foams, powders, conductors, insulators, solids, gases, etc.

WDM conditions are obtained by combined longitudinal and transverse space-charge neutralized drift compression [3] of the ion beam to provide a hot spot on target with a beam spot size of ~1 mm, and pulse length from microseconds to nanoseconds. Local temperatures approaching 0.5 eV (~6000 K) have been observed in thin (50-150nm) foil targets of Au, Si, Pt, and C [4].

Beam profile measurements at the target plane are used to tune the beam transport system to optimize the beam intensity onto target foils. Alumina (Al_2O_3) scintillators are employed since they have a linear response over a large dynamic range and are relatively resistant to dose-related damage, at least at lower intensities. At higher intensities, greater than ~200kW/cm^2, saturation or other nonlinear effects may limit the upper range of measurable beam intensity. To address these issues, we have adapted our target diagnostic suite to examine the uses of thick foils for beam calorimetry measurements.

Tungsten has the highest melting temperature (3420°C) of the refractory metals from atmospheric pressure to ultra-high vacuum conditions. It is commonly used in high temperature applications (wire filaments, etc.) where high tensile strength is required.

The specific heat capacity, c_p, of tungsten (~24.4 J/mol/K) measures the temperature change expected from beam irradiation. Temperature-dependent values of the specific heat capacity can be found in standard references [5-6].

For beam calorimetry we use a 3μm thick solid tungsten foil, in which 300kV potassium ions deposit their energy within the first 100nm. The resolution of the optical system is ~11.4pixel/mm, or a pixel size of 88μm. On this length scale, the foil is thin compared to the resolution limit. The thermal diffusion length over a time *t* is given by

$$\delta_{th} = 2\sqrt{\kappa t}\,, \qquad (1)$$

*This work was supported by the Director, Office of Science, Office of Fusion Energy Sciences, of the U.S. Department of Energy under Contract No. DE-AC02-05CH11231.

#SMLidia@lbl.gov

where κ is the diffusivity (~68 $\mu m^2/\mu sec$). Hence, the diffusion time over the pixel size is ~30μsec. This sets the upper time scale duration for resolvable processes. The diffusion time over the foil thickness is ~33ns. This sets the lower limit on temporal resolution. Within these limits, an instantaneous bulk heating or one-dimensional heat transport model provides an accurate approximation to the thermal dynamics.

PHYSICS OF THERMAL EMISSION

Blackbody radiation with emissivity

The Stefan-Boltzmann law [7] provides the basis for estimating the temperature of an object from its thermal radiation intensity:

$$P_{rad} = A\varepsilon\sigma_{SB}T^4, \qquad (2)$$

where P_{rad} is the total object irradiated power, A is the area of the radiating object held at a uniform temperature T, ε is the emissivity of the material, and σ_{SB} is the Stefan-Boltzmann constant. Direct observation of the 4th power law requires perfect detectors integrating across the entire spectrum. Real detectors will collect only a fraction of the spectrum, drastically altering the power law behavior to larger effective exponents.

Optical pyrometers are calibrated absolutely against NIST traceable radiation sources, eg. tungsten ribbon lamps, and measure intensity within a narrow wavelength band. Reconstructed temperature, T, can be obtained from a non-linear least-squares fit of measured spectra, $I(\lambda,T)$, to a radiation model. Using a Planck's Law model [7] with spectral emissivity ε(λ), the two-parameter fitting function is [8]

$$I(\lambda,T) = \varepsilon(\lambda)\frac{C_1}{\lambda^5}\left[e^{C_2/\lambda T} - 1\right]^{-1}. \qquad (4)$$

Tabulated emissivity data at 650nm is available [9].

Local temperature evolution

The local temperature in a material is governed by the interplay of heat fluxes and heat transport described by the one-dimensional heat equation:

$$\rho c_p \partial_t T = \partial_x\left(K\partial_x T\right) + S(x,t), \qquad (5)$$

where ρ is the material density and K is the conductivity. Here x defines the distance into the foil from the upstream side. The source term, S, describes the influx of beam ions impinging on the foil and depositing their kinetic energy within ~100nm. The boundary conditions can be written as

$$\left(K\partial_x T\right)_{U,D} = F_{U,D}(T), \qquad (6)$$

where the subscripts U,D refer to Upstream or Downstream, respectively, and F describes the various contributions to fluxes removing energy from the foil surfaces from evaporation, radiation, and thermionic emission. On the time and temperature scales of interest for the diagnostic, the cooling fluxes are neglected in the calculation of foil temperature.

Beam heating model

The one-dimensional heat transport equation has been modeled and solved numerically. Figure 1 shows the time evolution of the 3μm foil temperature under irradiation from a ~300-kV K^{+1} beam. A shelf in the temperature response is indicative of a material phase change.

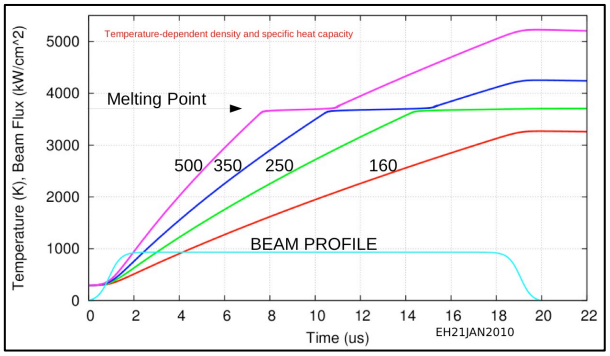

Figure 1: Temperature of the 3μm tungsten under prescribed ion beam irradiation.

EXPERIMENTAL RESULTS

The NDCX-I [10] facility generates a K^{+1} ion beam with kinetic energy 250kV-350kV, beam current 20-30mA, pulse duration ~3-20μsec, and repetition frequency ~0.05-0.1 Hz. Solenoid magnets are used for beam transport and envelope matching into a plasma-neutralized drift section. An 8 T final focus solenoid images the beam onto the target foil. Measured beam intensities >200kW/cm^2 are routinely produced.

Capacitive and resistive voltage dividers monitor the beam voltage, while Faraday cups provide beam current measurements. One hundred micron thick Al_2O_3 scintillators are used with gated, image-intensified 16-bit MCP cameras (Princeton Instruments PI-MAX) to image the beam profile. A fine metal mesh (biased to -300 V) prevents charge buildup on the scintillator. The ion beam deposits all its energy in the scintillator within 1μm. Horizontal and vertical slits are used with the scintillator or with a slit-Faraday cup to measure beam phase space. The target plane is instrumented with a scintillator and a camera (88μm resolution), and the Fast Faraday Cup with ~1ns temporal resolution.

Target diagnostics include a fiber-coupled relay lens light collection system (200μm probing spot) coupled to an absolutely calibrated, time-resolved streak-camera-based spectrometer (Hamamatsu C7700) or a four-band fast optical pyrometer [11]. A downstream fast current transformer (Bergoz FCT-016-20:1-VAC) captures the transmitted beam current at the target plane after the foil target spot melts and material is removed.

Beam profile tuning and energy variation

The ion beam transverse profile at the target plane was obtained using the gated camera (80mm, f/1.4, 2x teleconverter) with the scintillator and tungsten foils. Figure 2 shows the variation in beam profile as the beam energy was varied. The beam duration and camera gate was 5μsec. The final focus solenoid was held fixed at 8 T, while the upstream optics are adjusted to maintain energy-independent transverse beam envelopes and beta-functions. In the scintillator cases, the camera gain was 250 and the peak pixel value was ~23000, while in the foil cases the camera gain was 50 and the peak pixel value was ~15000. Under the same irradiation for 5μsec, the foil presents a much brighter radiation source.

The foil emission displays much greater sensitivity to the peak of the beam distribution than does the scintillator, but radiates much of its total power outside of the camera detector's spectral sensitivity range. The central core of the beam is peaked and generates a peaked irradiation profile. While scintillators exhibit nearly linear fluorescence intensity to energy deposition, the thermal emission intensity of the foil is highly nonlinear and follows a Planck intensity distribution, as shown in Eqn 4.

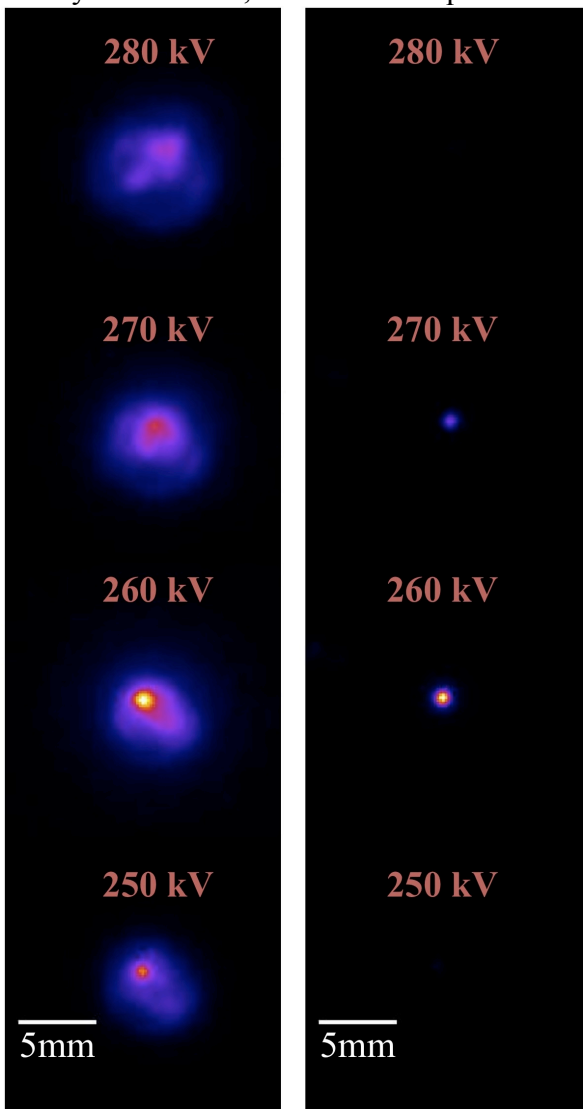

Figure 2: Scintillator (left) and tungsten foil (right) false color images of 5μsec beam irradiation. Peak intensity is white.

Normalized horizontal cross-sections of the 260kV beam energy scintillator and foil image profiles are shown in Figure 3. The raw foil intensity distribution is corrected via

$$I_{corr} = I_{raw}^{1/n}, \qquad (7)$$

where the exponent n is chosen so that the foil intensity profile width matches that of the

scintillator. A best-fit match reveals $n = 9 \pm 1$, for a 1.05mm FWHM.

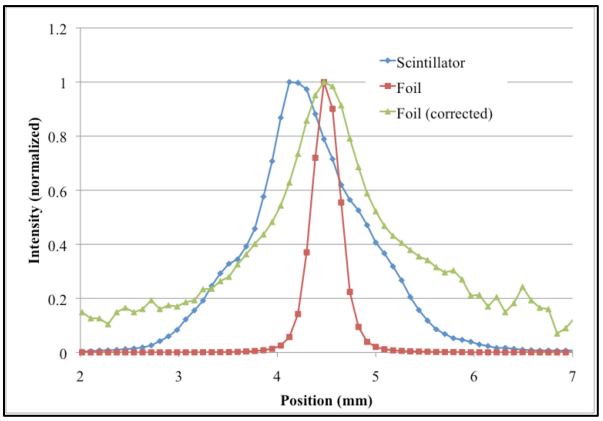

Figure 3: Horizontal cross-sections of scintillator and foil images of the 260kV beam.

Using this correction scaling, the variation of the peak intensity with beam energy is analyzed. Figure 4 shows the measured and the corrected intensities. Factors of ~100 in measured intensity indicate only a factor of ~2 in true intensity variation over the range of beam energies scanned.

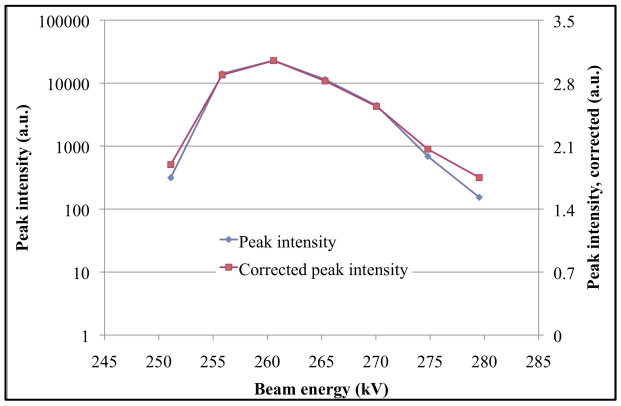

Figure 4: Measured and corrected peak intensity versus irradiating beam energy.

Beam Intensity from Scintillator Profile

The beam intensity profile is obtained from cross-calibration of the scintillator image with the beam power, obtained from beam voltage measurements and beam current in the target chamber Fast Faraday Cup. These are average values obtained over multiple shots. The calibrated beam intensity is shown in Figure 5 for a 260 kV beam energy, and 5.6 kW beam power over the 5µsec pulse duration. The peak beam intensity is estimated at ~248 kW/cm^2, based on scaling the total beam power to the entire acquired image distribution. Any hypothesized intensity-dependent saturation effects will only affect the peak valued pixel(s).

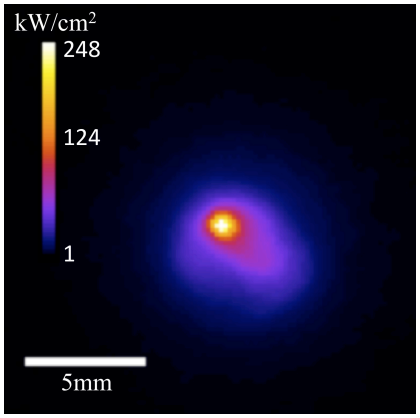

Figure 5: Calibrated beam intensity for 260kV beam energy, measured with the scintillator.

Foil Temperature from Optical Pyrometry

The calibrated streak-spectrometer was used to analyze the thermal emission at 650nm from the foil during and after beam irradiation (beam power 5.6kW, pulse duration ~10µsec). The foil spot temperature is calculated from Eqn. 4 assuming a spectral emissivity ε_{650nm} ~0.43. Signal to noise limits the detector's lower temperature threshold to ~1700K. Temperature error bars (+300K -150K) are estimated based on the relative uncertainty of the emissivity. The reconstructed temperature response is shown in Figure 6, averaged over 20 shots.

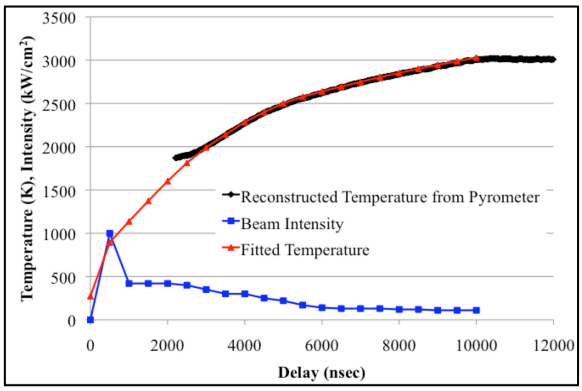

Figure 6: Measured foil temperature, estimated beam intensity and calculated foil temperature from pyrometer data.

Beam Intensity from Optical Pyrometry

Beam intensities were estimated by assuming a uniform irradiance over the 200µm analyzing fiber aperture, and then matching the calculated foil temperature rise to the reconstructed pyrometer temperature. The heat equation, Eqn. 5, was solved numerically, and the results are presented in Figure 6. The average beam intensity is estimated to be 430 kW/cm^2 between 0 and 4 µsec, 133 kW/cm^2 between 4 and 10 µsec, and 260 kW/cm^2 between 0 and 10 µsec. This matches the predictions from the 1D thermal model (Figure 1) over the initial 4-5µsec beam heating period.

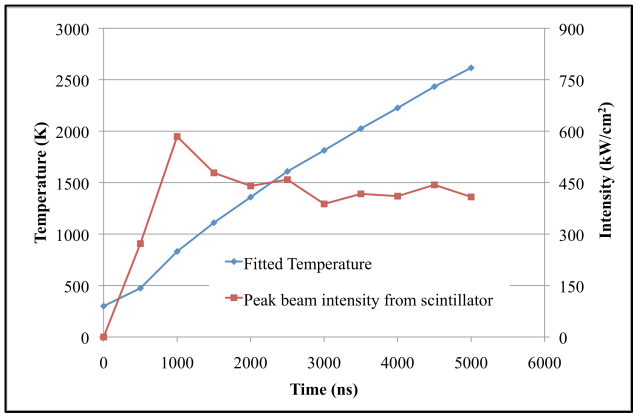

Figure 7: Renormalized peak beam intensity and calculated foil temperature.

Cross-calibration of Scintillator Beam Intensity

The scintillator intensity response is known to degrade and to possibly saturate under high beam irradiance. The peak beam intensities from time-resolved scintillator measurements are corrected to generate the measured temperature rise in the tungsten foil. A cross-calibration factor of 2.2 applied to the measured scintillator peak beam intensity generates the same foil temperature rise (to ~2400 K) by direct integration of Eqn. 5 over the ~5µsec beam pulse duration, shown in Figure 7. This results in a cross-calibrated peak beam intensity ~430kW/cm^2, averaged over the 5µsec beam pulse duration. This is to be compared with the measured peak intensity 248 kW/cm^2 obtained using only the scintillator and Faraday cup (Figure 5). In this case, the correction factor would be ~1.7. Hence, we see that there exists an empirical correction factor ~2 to be applied to the peak beam intensity derived solely from scintillator and Faraday cup measurements, and that this factor is an estimate to the degree of saturation of these beams in thin alumina scintillator wafers.

CONCLUSIONS

We have described a novel diagnostic capability that extends the dynamic range of scintillator-based beam profile measurements for intense ion beam characterization. We have described an empirical procedure to estimate the degree of saturation and deviation from linearity in scintillator materials. Calorimetric measurements support peak ion beam intensities of 430kW/cm^2 over a 200µm spot. This matches well with 1-D dynamic heating models.

REFERENCES

[1] J.J. Barnard, *et al*., Proc. 2005 Particle Accelerator Conference, p.2568.

[2] P.K. Roy, *et al*., *Nucl. Instrum. Methods Phys. Res.* **A** 577 (2007) 223-230.

[3] P.A. Seidl, et al., *Nucl. Instrum. Methods Phys. Res.* **A** 577 (2007) 215-222.

[4] F. Bieniosek, *et al*., Proc. Sixth Intl. Conf. on Inertial Fusion Sciences and Applications (IFSA2009), IOP Press.

[5] R.C. Weast (ed.), CRC Handbook of Chemistry and Physics, CRC Press, Inc., 1984.

[6] G.K.White and S.J. Collocott, *J. Phys. Chem. Ref. Data* **13** (1984) 1251-1257.

[7] See, for example, C. Kittel and H. Kroemer, Thermal Physics, W.H. Freeman and Company, 1980.

[8] P.A. Ni, *et al*., *Laser and Particle Beams*, December 2008.

[9] R.D. Larrabee, *J. Opt. Soc. Am.* **49** (1959) 619-625.

[10] S.M. Lidia, *et al*., Proc. 2009 Particle Accelerator Conference, TU6PFP092.

[11] P.A. Ni, *et al*., *Nucl. Instrum. Methods Phys. Res.* **A** 606 (2009) 169-171.